

Imaging characterization of multifocal pediatric bony lesions

Mindy X. Wang, MD; Nicholas Bates, MD; Tarik Nurkic, MD; and Dhanashree Rajderkar, MD

A multitude of benign bony lesions are recognized in the pediatric age group. Many of these lesions frequently have a characteristic appearance and do not require further workup. Knowing the appearance of these lesions can guide effective utilization of the tools radiologists have at their disposal and can often obviate the need for unnecessary biopsies and their potential complications. Herein, we review the characteristic appearances of multifocal bony lesions in 14 diseases and conditions that afflict the pediatric population.

Langerhans cell histiocytosis

Langerhans cell histiocytosis (LCH) is a neoplastic proliferation of

Langerhans cells. Although it is most frequently monoostotic, it can be polyostotic in 25-34% of patients. Bone lesions are the most common radiographic manifestation of LCH (Figure 1), occurring in 80% of patients. "Punched-out" lesions with a beveled edge are often seen in the skull.¹ Vertebra plana and "floating teeth" may be seen in the mandible, ribs, pelvis and spine.^{1,2} In long bones, endosteal scalloping may be responsible for a "budding" appearance.² Bony involvement in children with LCH can resemble multiple myeloma in the adults.² On MRI, the lesion is usually isointense on T1, predominantly hyperintense on T2 and shows marked contrast enhancement. MRI helps in delineating

the soft tissue component.² LCH may require biopsy for confirmation of the pathology and can be a close mimicker of some of the malignant processes. The same can be said of polyarteritis nodosa and chronic recurrent multifocal osteomyelitis, which are also discussed in this article.

Renal osteodystrophy

Renal osteodystrophy occurs in chronic renal failure due to osteomalacia/rickets and secondary hyperparathyroidism. Imaging findings include demineralization, osteosclerosis, soft tissue and vascular calcifications, and brown tumors.³ Demineralization can be subperiosteal, endosteal, subchondral, subligamentous and along the joint margins. Subperiosteal resorption is often seen on the radial aspects of the middle phalanges in the index and long fingers.³ (Figure 2) "Rugger jersey spine" indicates the sclerosis of vertebral body endplates with alternating bands of different density.³

Bone infarct/osteonecrosis

The most common causes of bone infarct or osteonecrosis include trauma, corticosteroids, sickle cell disease and idiopathic. Common sites of involvement include the femoral and humeral

Dr. Wang is an Internal Medicine preliminary year resident at University of Florida and will pursue Diagnostic Radiology training at University of Texas Health Science Center at Houston; Dr. Bates and Dr. Nurkic are Diagnostic Radiology residents at University of Florida; and Dr. Rajderkar is a Professor of Radiology at the University of Florida College of Medicine, Gainesville, FL, 32608. Conflicts and disclaimers: Dr. Rajderkar was the recipient of a Toshiba Putting Patients First Grant for "Making ALARA More Meaningful and Achievable in GI/GU Fluoroscopy." Dr. Rajderkar was a principal researcher on IBP-9414-010: A randomized, double blind, parallel group, dose escalation placebo-controlled multicenter study to investigate the safety and tolerability of IBP-9414 administered in preterm infants.

Prior presentation: This article is adapted from: Bates N, Nurkic T, D. Rajderkar. Spectrum of fascinating benign bony lesions – A complete review of multifocal bony benign lesions in pediatric age group. Presented as an Educational exhibit at Society of Pediatric Radiology; April 2016; Bellevue, WA.

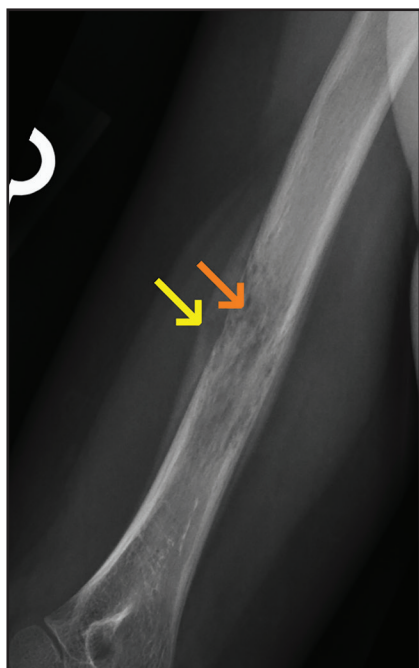
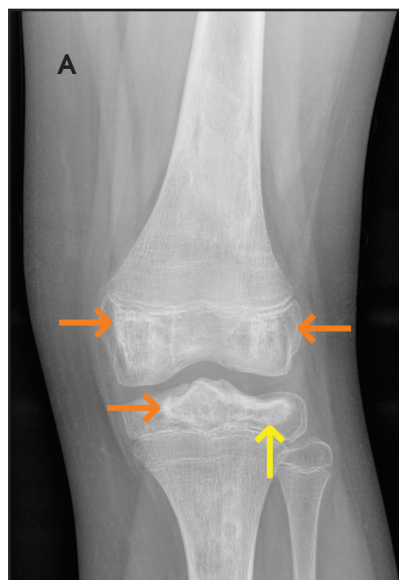


FIGURE 1. Permeative, aggressive-appearing lesion centered in the right humeral diaphysis (orange arrow) associated with extensive, smooth periosteal reaction (yellow arrow).



FIGURE 2. X-ray of the hand demonstrates multiple brown tumors (orange arrows).



senting subchondral collapse. (B) Corresponding T1 SE and PD coronal MR image of the same patient demonstrate multiple bone infarcts with serpiginous margins with increased T2 signal (orange arrows).



FIGURE 3. AP radiograph (A) of the knee demonstrating multiple bone infarcts (orange arrows) involving the metadiaphysis and epiphysis of the distal femur and proximal tibia. The bone infarct in the left lateral tibial condylar epiphysis (yellow arrow) is associated with a concavity of the articular surface likely representing subchondral collapse.

heads, knee, femoral/tibial metadiaphysis (Figure 3), scaphoid, lunate and talus.⁴ Diagnostic signs include a serpentine rim of sclerosis on radiographs. Photopenia is seen in early disease on bone scintigraphy. A maintained yellow marrow with a serpentine rim of high signal intensity on MRI is typical.⁴ These

imaging features reflect the body's underlying response to wall off the osteonecrotic process.

Hemophilic arthropathy

Hemophilic arthropathy is caused by repeated bleeding into the synovial joints, commonly the knee (Figure 4),

ankle, elbow, and shoulder.⁵ The bleeding may extend into muscles or bones causing joint contractures or soft tissue pseudotumors and osseous pseudotumors.⁵ Imaging findings include hemarthrosis; synovial inflammation and hyperemia; chondral erosions and subchondral resorption with osseous erosions and cyst formation; joint space narrowing due to cartilage loss; intraosseous or subperiosteal hemorrhage; sclerosis; and osteophytosis.⁵ Hypertrophied synovial membrane is seen with low signal intensity on MR on all sequences due to the magnetic susceptibility caused by hemosiderin.

Tuberous sclerosis

Spontaneous mutations account for most cases (56-80%) of tuberous sclerosis, while the remainder are inherited as autosomal dominant traits.⁶ Manifestations involve multiple organ systems, including the bone, although less frequently involved. Bony manifestations include cystic lesions, hyperostosis of the inner table of the calvaria, osteoblastic changes, periosteal new bone and scoliosis.⁷ While the lesions can occur anywhere in the bone, the most common locations are the calvaria, short tubular bones of the hand or foot, spine, and pelvis (Figure 5).⁷

Neurofibromatosis I

Neurofibromatosis I is one of the most common genetic diseases, occurring in 1 of every 2,000 live births.⁸ This autosomal dominant disorder is due to a mutation or deletion of the NF1 gene on chromosome 17. Neurofibromin, the gene product, acts as a tumor suppressor and is important in skeletal development and growth. NF1 is characterized by the formation of neurofibromas and abnormalities related to mesodermal dysplasia. Multiple organ systems, with skeletal abnormalities (Figure 6), are seen in up to 50% of patients. Typically, the skeletal abnormalities include focal thoracic scoliosis, posterior scalloping of the vertebral bodies, thinning of the ribs, wide neural foramina and sphenoid wing hypoplasia. Hemihypertrophy and

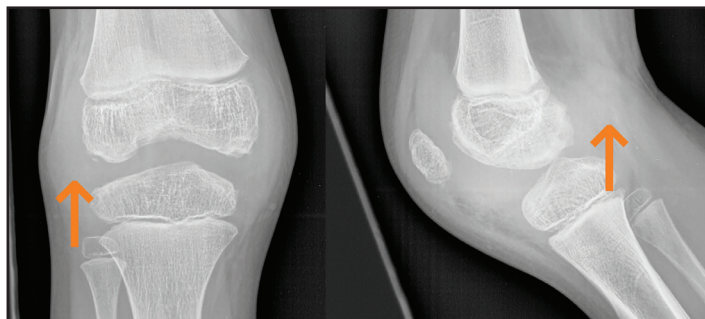


FIGURE 4. Radiograph shows dense joint effusion of the right knee (orange arrows).

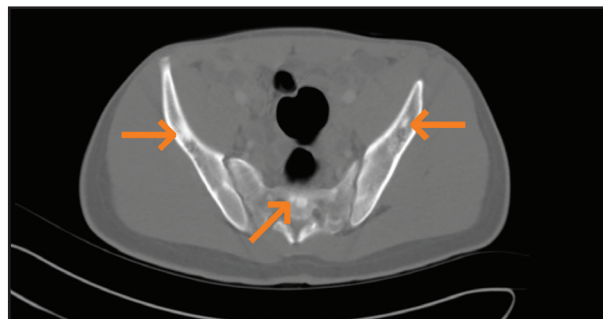


FIGURE 5. Axial CT slice demonstrating multiple sclerotic lesions (orange arrows) involving pelvis and sacrum.

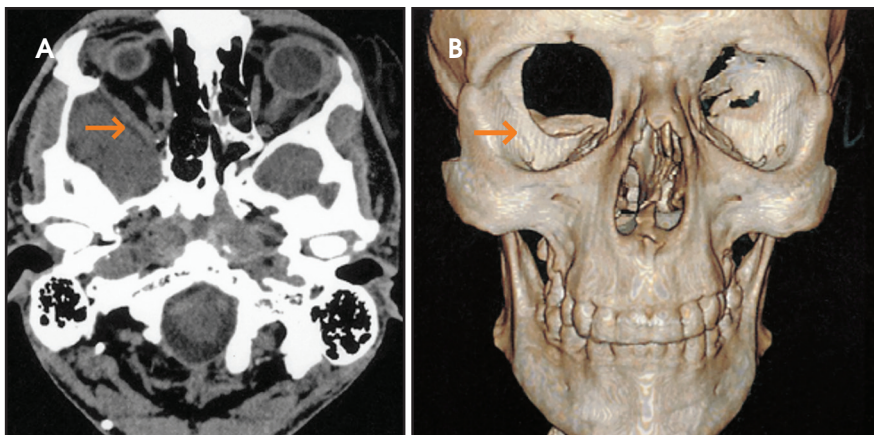


FIGURE 6. CT scan showing absent greater wing of the sphenoid (A, orange arrow) causing bare orbit appearance (orange arrow) on reconstruction (B).

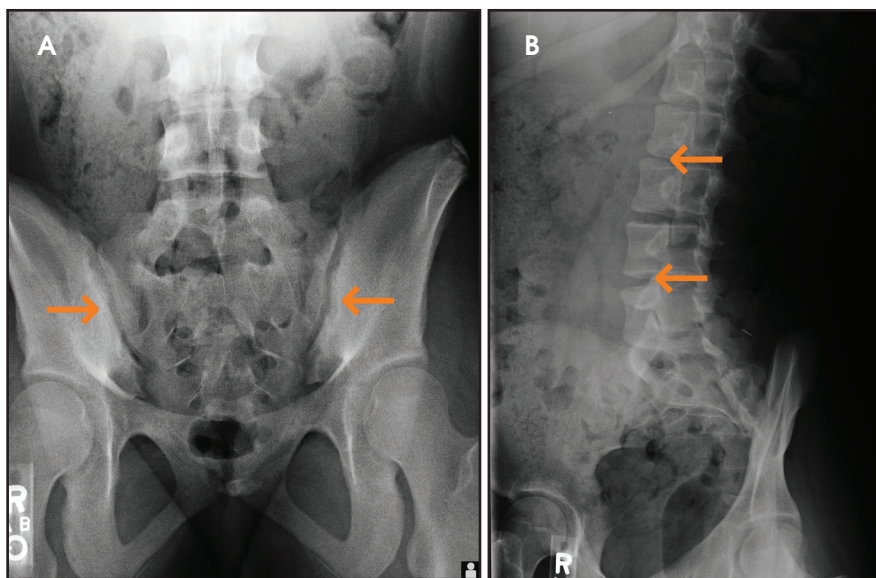


FIGURE 7. Bilateral sacroiliitis (A, orange arrows); findings typical for healed erosions at the anterior superior corners of the L3-L5 vertebral bodies (B, orange arrows).

tibial and fibular pseudarthrosis are also encountered.⁸

Spondyloarthropathy

Spondyloarthropathy includes ankylosing spondylitis, reactive arthritis,

spondylitis associated with inflammatory bowel disease, and psoriatic arthritis. The axial skeleton and sacroiliac joints are involved in most cases (Figure 7). In this location, findings include sclerosis and reduced articular space,

loss of definition of articular margins, subchondral osteoporosis, erosions, and widening of joint space and ankylosis.⁹ Active inflammation can be seen on MR imaging; bone marrow edema is periarthritic and demonstrates increased signal on fat-saturated T2 or STIR images and enhancement on fat-saturated T1 images.⁹ Synovitis is seen as enhancement in the synovial part of the joint. Capsulitis and enthesitis manifest as increased signal on STIR, fat-suppressed T2, and contrast-enhanced images.

Chronic recurrent multifocal osteomyelitis (CRMO)

Chronic recurrent multifocal osteomyelitis (CRMO) can affect any skeletal site; however, there is predilection for certain locations. These locations are unusual when compared with infectious osteomyelitis; locations include tubular bones, clavicles (Figure 8), and less frequently spine and pelvic bones.¹⁰ Radiographs demonstrate lytic lesions with a sclerotic rim, which predominantly affect metaphyses of tubular bones with symmetric involvement.¹⁰ The sclerotic rim is the most characteristic radiographic feature. Clavicular lesions demonstrate lytic medullary destruction of the medial clavicle.¹⁰ On MRI, decreased T1 signal and increased signal on susceptibility imaging, T2, and STIR sequences represent bone marrow edema. These sites typically do not involve entheses, and there is no evidence of tenosynovitis as seen with juvenile idiopathic arthritis. These areas of increased STIR and T2 signal gradually disappear as normal bone marrow regenerates. There is inhomogeneous



FIGURE 8. Abnormal signal uptake at multiple sites, including medial clavicles, proximal right femur, and T6 vertebral body (orange arrows).

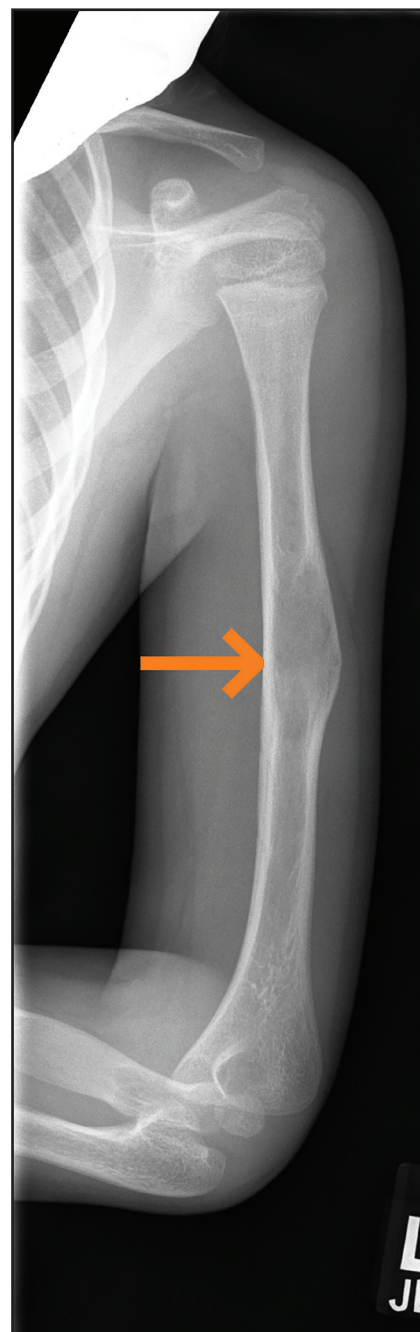


FIGURE 9. Expansile groundglass lesions in the mid left humerus (orange arrow).

enhancement typically involving the sites of bone marrow edema.

Polyostotic fibrous dysplasia

Polyostotic fibrous dysplasia is a non-inherited osseous disease in which abnormal osteoblasts replace normal marrow with cancellous immature bone. This is often unilateral involv-

ing larger segments of long bones and is frequently clinically apparent when the patient presents with pathologic fractures.¹¹ Radiographs demonstrate intramedullary, expansile, well-defined lesions (Figure 9). A smooth cortical contour is always maintained and may appear completely radiolucent or sclerotic.¹¹ A hazy internal matrix is noted

on radiographs. Bone scan demonstrates nonspecific uptake of radio-tracer. MRI demonstrates a variable appearance with low to intermediate T1 signal intensity. T2 signal intensity is variable and usually heterogeneous and can range from low to intermediate to high. This is thought to be secondary to the fibrous components of the lesions.

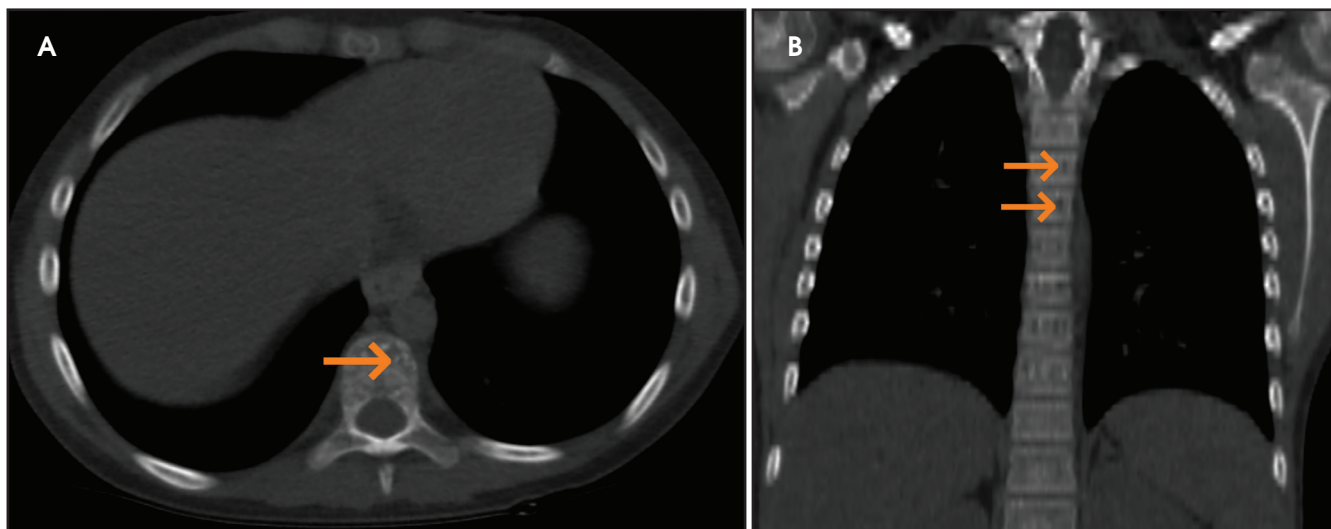


FIGURE 10. Lucent lesions (A, orange arrow) most consistent with intraosseous hemangiomas within the T9 and T10 vertebral bodies. Multi-level lucent lesions within the thoracic vertebral bodies most consistent with intraosseous hemangiomas (B, orange arrows).

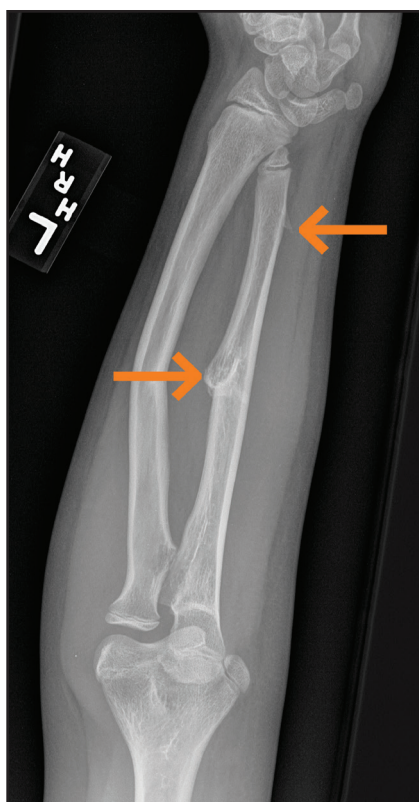


FIGURE 11. Pedunculated osteochondroma of the left ulna (orange arrows).

High T2 signal is noted with cystic change of fibrous dysplasia lesions.

Multifocal intraosseous hemangiomas

Multifocal intraosseous hemangiomas are usually incidental findings in

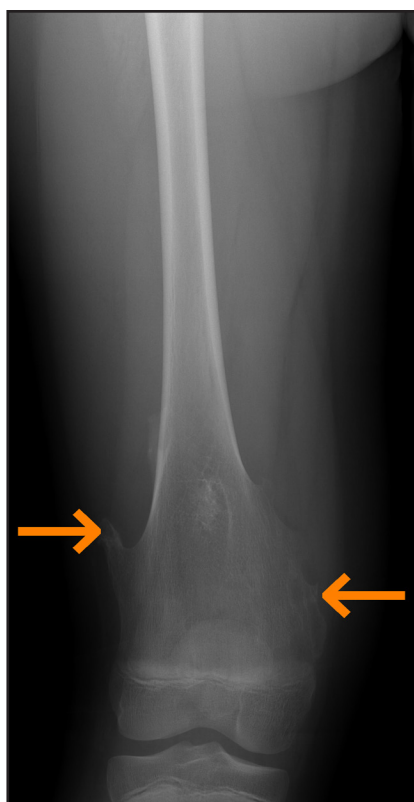


FIGURE 12. Pedunculated and sessile osteochondromas of the distal right femoral metadiaphysis (orange arrows).

the skull or spine. These are slow-growing benign vascular malformations. The most common locations include vertebral column and frontal/parietal bones.¹² Radiographs demonstrate lucent lesions with sclerotic rims and a honeycomb or “sunburst” trabecular

pattern. Vertebral lesions demonstrate prominent vertical trabeculae, the “corduroy” sign. CT demonstrates findings similar to radiographs with lucent lesions (Figure 10) and sclerotic borders. MRI reveals a well-circumscribed mass with intra- and extracranial extension. Hemangiomas typically demonstrate T1 shortening as a result of their intralesional fat content. These lesions demonstrate markedly increased signal on T2 sequences and heterogeneous enhancement.¹²

Multiple hereditary exostoses

Multiple hereditary exostoses are bony dysplasias consisting of osteochondral exostoses. Osteochondromas are the most common benign bone tumors comprising 35% of benign bone tumors.¹³ These are seen as sessile or pedunculated lesions (Figure 11) affecting the distal femoral metadiaphysis (Figure 12) on imaging. Radiographs demonstrate continuity with the medullary cavity of the lesion with the parent long bone. MRI demonstrates continuity of the cortices and medullary cavities of the osteochondroma with the parent bone. The cartilage cap demonstrates high T2 signal intensity. The internal marrow and cortex signal should match the signal of the parent long bone. Malignant degeneration to chondrosarcoma may occur and may



FIGURE 13. Squaring and proximal tapering of the metatarsal bones (A, orange arrow), radius, and ulna (B, orange arrow).



FIGURE 14. Plain (lateral) radiograph of the right upper extremity revealing diffuse periosteal thickening of both the bones of the forearm (orange arrows).

be characterized as thickening of the cartilage cap more than 2 cm in thickness. MRI evaluates soft tissue sequelae from osteochondroma including soft tissue edema, neurovascular impingement, and



FIGURE 15. MRI T2-weighted images of the right forearm demonstrate marked diffuse, circumferential periosteal thickening involving the radius and ulna (orange arrow). In addition, marked soft tissue involvement including the muscular compartment consistent with myositis (yellow arrow).

bursitis. Osteochondromata demonstrate increased uptake with bone scanning agents at site of bone growth.¹⁴ Increased

uptake discontinues as the lesion stops growing unless the lesion has undergone malignant degeneration.

Glycogen storage disorders

Hurler's syndrome or Mucopolysaccharidosis type II is pan-ethnic glycogen storage disease with an incidence of 1 in 88,000.¹⁵ Characteristic radiographic findings demonstrate antero-inferior beaking of the vertebral bodies. Additional findings include "step-off" deformity and broadening of the metacarpals with thickening of the phalanges (Figure 13). Mild kyphosis of the thoracolumbar junction is typically present.¹⁶ MRI demonstrates narrowing of the foramen magnum secondary to thickening of the atlanto-occipital ligaments and dysplastic odontoid. In extreme cases this can result in narrowing of the spinal canal and cord compression.

Polyarteritis nodosa

Polyarteritis nodosa (PAN) is included in the category of necrotizing vasculitis. Most cases in radiology literature are based on vascular findings. Cases of periostitis in patients with PAN,¹⁷ are usually found in cases of relapse of disease. Roughly 50% of children present with musculoskeletal symptoms including joint, muscle or

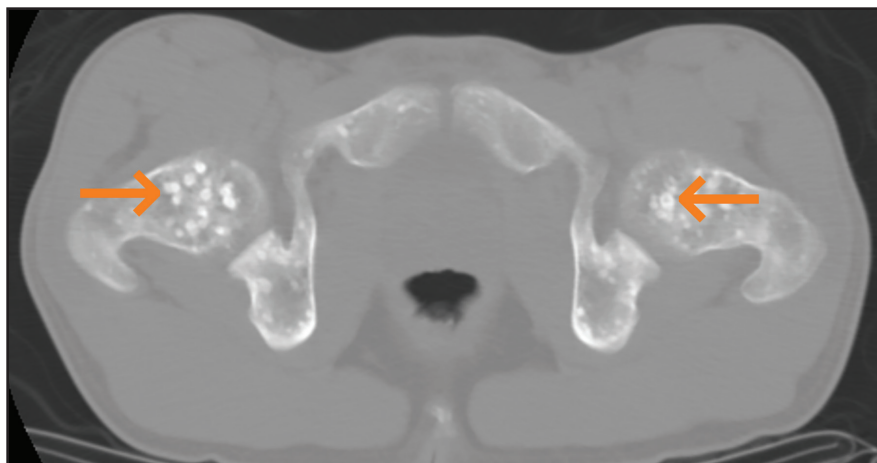


FIGURE 16. CT demonstrating multiple 'bone islands' (orange arrows) involving the proximal femurs.

limb pain upon initial diagnosis.¹⁷ Radiographs typically demonstrate periosteal reaction (Figures 14, 15), which most often affects the long bones of the legs and may or may not be accompanied by cutaneous lesions. Bone scan demonstrates increased uptake in the region of the periostitis. Biopsy is usually required to rule out the aggressive cancers.

Osteopoikilosis

Osteopoikilosis, also called "spotted bone disease," is a rare, benign, autosomal dominant disorder. The pathognomonic appearance includes sclerotic bone lesions most commonly involving the hands, feet, pelvis, and ends of long bones in a symmetric distribution, especially around the joints. Radiographically these lesions typically are aligned with the bony trabeculae and demonstrate mildly spiculated margins. The lesions are usually asymptomatic and incidentally found giving the appearance of 'multiple bone islands' (Figure 16). The enostoses demonstrate decreased signal on both T1 and T2 sequences. The disease can be associated with dermatofibrosis and lenticularis

disseminata. Differential diagnoses include osteoblastic metastases, tuberous sclerosis and mastocytosis.¹⁸

Conclusion

Benign bony lesions in children can be congenital or acquired, and the acquired conditions may be infectious, inflammatory or neoplastic. Characterizing them using the appropriate radiologic modality is essential for successful management. Characteristic appearance of fibrous dysplasia, multiple hereditary exostoses, osteopoikilosis, and hemangiomas warrant no additional investigations or follow up. However, lesions like neurofibromatosis I, tuberous sclerosis and renal osteodystrophy may require additional workup if the underlying conditions are not unknown; otherwise, these lesions do not need further workup. Lesions such as LCH, CRMO, and spondyloarthropathy can have varied appearance and would need thorough workup.

REFERENCES

1. Zaveri J, La Q, Yarmish G, Neuman J. More than just Langerhans cell histiocytosis: a radiologic review of histiocytic disorders. *Radiographics*. 2014;34(7):2008-2024.

2. Khung S, Budzik JF, Amzallag-bellenger E, et al. Skeletal involvement in Langerhans cell histiocytosis. *Insights Imaging*. 2013;4(5):569-579.
3. Lim CY, Ong KO. Various musculoskeletal manifestations of chronic renal insufficiency. *Clin Radiol*. 2013;68(7):e397-411.
4. Murphey MD, Foreman KL, Klassen-fischer MK, et al. From the radiologic pathology archives imaging of osteonecrosis: radiologic-pathologic correlation. *Radiographics*. 2014;34(4):1003-1028.
5. Llauger J, Palmer J, Rosón N, et al. Nonseptic monoarthritis: imaging features with clinical and histopathologic correlation. *Radiographics*. 2000; 20 Spec No:S263-S278.
6. Logue LG, Acker RE, Sienko AE. Best cases from the AFIP: angiomyolipomas in tuberous sclerosis. *Radiographics*. 2003;23(1):241-246.
7. Umeoka S, Koyama T, Miki Y, et al. Pictorial review of tuberous sclerosis in various organs. *Radiographics*. 2008;28(7):e32.
8. Fortman BJ, Kuszyk BS, Urban BA, et al. Neurofibromatosis type 1: a diagnostic mimicker at CT. *Radiographics*. 2001;21(3):601-612.
9. Navallas M, Ares J, Beltrán B, et al. Sacroiliitis associated with axial spondyloarthropathy: new concepts and latest trends. *Radiographics*. 2013;33(4):933-956.
10. Jurik AG. Chronic recurrent multifocal osteomyelitis. *Semin Musculoskelet Radiol*. 2004;8(3): 243-253.
11. Fitzpatrick KA, Taljanovic MS, Speer DP, et al. Imaging findings of fibrous dysplasia with histopathologic and intraoperative correlation. *AJR Am J Roentgenol*. 2004;182(6):1389-1398.
12. Politi M, Romeike BF, Papanagiotou P, et al. Intraosseous hemangioma of the skull with dural tail sign: radiologic features with pathologic correlation. *AJNR Am J Neuroradiol*. 2005;26(8): 2049-2052.
13. Lee KC, Davies AM, Cassar-Pullicino VN. Imaging the complications of osteochondromas. *Clin Radiol*. 2002;57(1):18-28.
14. Epstein DA, Levin EJ. Bone scintigraphy in hereditary multiple exostoses. *AJR Am J Roentgenol*. 1978;130(2):331-333.
15. Pastores GM, Meere PA. Musculoskeletal complications associated with lysosomal storage disorders: Gaucher disease and Hurler-Scheie syndrome (mucopolysaccharidosis type I). *Curr Opin Rheumatol*. 2005;17(1):70-78.
16. Kumar R, Guinto FC, Madewell JE, et al. The vertebral body: radiographic configurations in various congenital and acquired disorders. *Radiographics*. 1988;8(3):455-485.
17. Carron P, Hoffman IE, De Rycke L, et al. Case number 34: Relapse of polyarteritis nodosa presenting as isolated and localised lower limb periostitis. *Ann Rheum Dis*. 2005;64(8): 1118-1119.
18. Negi RS, Manchanda KL, Sanga S, et al. Osteopoikilosis - Spotted bone disease. *Med J Armed Forces India*. 2013;69(2):196-198.